Title: Characterization of a novel endopeptidase Cwl0971 that hydrolyzes peptidoglycan of *Clostridioides difficile* involved in pleiotropic cellular processes

Running title: Cwl0971 plays key roles in *C. difficile*

Duolong Zhu[1], Hiran Malinda Lamabadu Warnakulasuriya Patabendige[1], Brooke Rene Tomlinson[2], Shaohui Wang[1], Domenica Flores[1], Yongqun He[3], Lindsey N Shaw[2], Xingmin Sun[1]*

[1]Department of Molecular Medicine, Morsani College of Medicine, University of South Florida, Tampa, FL, United States.

[2]Department of Cell Biology, Microbiology and Molecular Biology, University of South Florida, Tampa, Florida, USA.

[3]Department of Microbiology and Immunology, and Center for Computational Medicine and Bioinformatics, Unit for Laboratory Animal Medicine, University of Michigan Medical School, Ann Arbor, MI, USA.

* Corresponding author.

Address: 12901 Bruce B. Downs Blvd Tampa, FL 33612, United States

Fax: +1-8139747357

E-mail: sun5@usf.edu

Phone: Phone: +1-8139744553

Summary

Clostridioides difficile is a Gram-positive, spore-forming, toxin-producing anaerobe that can cause nosocomial antibiotic-associated intestinal disease. Although the production of toxin A (TcdA) and toxin B (TcdB) contribute to the main pathogenesis of *C. difficile*, the mechanism of TcdA and TcdB release from intracell remains unclear. In this study, we identified and characterized a new cell wall hydrolase Cwl0971 (endopeptidase, CDR20291_0971) from *C. difficile* R20291, which is involved in bacterial autolysis. The gene *0971* deletion mutant (R20291Δ0971) generated with CRISPR-AsCpfI exhibited significantly delayed cell autolysis and increased cell viability compared to R20291, and the purified Cwl0971 exhibited hydrolase activity for *Bacillus subtilis* cell wall. Meanwhile, 0971 gene deletion impaired TcdA and TcdB release due to the decreased cell autolysis in the stationary / late phase of cell growth. Moreover, biofilm formation, germination, and sporulation of the mutant strain decreased significantly compared to the wild type strain. *In vivo*, the depletion of Cwl097 decreased fitness over the parent strain in a mouse infection model. Collectively, Cwl0971 is involved in cell wall lysis and cell viability, which can affect several phenotypes of R20291. Our data indicate that the endopeptidase Cwl0971 is an attractive target for *C. difficile* infection therapeutics and prophylactics.

Introduction

Clostridioides difficile is a Gram-positive, spore-forming, toxin-producing, anaerobic bacterium that has established itself as a leading cause of nosocomial antibiotic-associated diarrhea in the developed countries (Sebaihia et al., 2006). *C. difficile* infection (CDI) can result in a spectrum of symptoms, ranging from mild diarrhea to pseudomembranous colitis and potential death (Lessa et al., 2012). Recently, morbidity and mortality rates of CDI have been increasing steadily, causing over 500,000 infections per year in the United States alone with an estimated cost of $1-3 billion (Dubberke and Olsen, 2012; Lessa et al., 2015). *C. difficile* has many virulence factors, such as toxins, adhesins, flagella, and proteases (Borriello et al., 1990; Janoir, 2016). Among them, two large potent exotoxins, toxin A (TcdA) and toxin B (TcdB) are the most well-studied virulence factors (Kuehne et al., 2010). These toxins can disrupt the actin cytoskeleton of intestinal epithelial cells through glucosylation of the Rho family of GTPases to induce mucosal inflammation and the symptoms associated with CDI (Voth and Ballard, 2005).

The toxin encoding genes *tcdA* and *tcdB* are located in a 19.6 kb pathogenicity locus (PaLoc), which also contains three additional genes, *tcdR*, *tcdC*, and *tcdE* (Braun et al., 1996; Mani and Dupuy, 2001). The gene *tcdR* encodes an RNA polymerase sigma factor that positively regulates the expression of both toxin genes and its own gene (Mani et al., 2002). TcdC is an antagonist of TcdR that negatively regulates TcdR-containing RNA polymerase holoenzyme (Dupuy et al., 2008). TcdA and TcdB belong to the large clostridial glycosylating toxin family, which are released without signal peptide (Popoff and Bouvet, 2009). TcdE, the holin-like protein, has been reported as being involved in toxin release (Govind and Dupuy, 2012; Govind

et al., 2015). However, the results of TcdE studies from different groups are controversial. Olling et al. (Olling et al., 2012) reported that toxin release from *C. dificile* 630Δ*erm* is not affected by *tcdE* gene mutation and indicated that transfer of *tcdE* gene into other microorganisms could lead to spontaneous lysis of the recipient. Recently, Wydau-Dematteis et al. (Wydau-Dematteis et al., 2018) characterized Cwp19, a novel lytic transglycosylase, which contributes to toxin release through bacteriolysis. In our previous study, we identified a novel peptidoglycan cross-linking enzyme Cwp22, which is involved in *C. difficile* cell wall integrity and can affect toxin release (Zhu et al., 2019). A link between toxin release and cell wall hydrolase-induced bacteriolysis needs further investigation to uncover the toxin secretion mechanism.

The bacterial cell wall has been reported to be involved in the central roles of bacterial physiology (Thwaites and Mendelson, 1991; Dmitriev et al., 2005). Peptidoglycan (PG), an essential cell wall biopolymer, is a primary cell wall constituent of Gram-positive bacteria formed by glycan strands of β-1,4-linked-N-acetylmuramic acid (NAM) and N-acetylglucosamine (NAG), cross-linked by short peptides attached to NAM (Layec et al., 2008). PG is a dynamic macromolecule and the constant equilibrium of PG in the cell is strictly controlled to enable bacterial growth and differentiation (Layec et al., 2008). Peptidoglycan hydrolases (PGHs, including bacteria autolysins) contribute to PG plasticity for maintaining cell wall shape through hydrolyzing PG bonds (Layec et al., 2008). According to the substrate specificity and the resulting cleavage products, PGHs can be defined into 5 classes as follows: N-acetylmuramoyl-L-alanine amidases (also named as amidases) which cleave the amide bond between the lactic acid side chain of NAM and L-alanine; carboxypeptidases which cleave the C-terminal amino acids of peptide chains; endopeptidases which cleave short peptides or cross-bridges; N-acetylglucosaminidases and N-acetylmuramidases (lysozyme and transglycosylases

included) which both can cleave β-1,4-bonds between disaccharide units of peptidoglycan (Layec et al., 2008; Vollmer et al., 2008). Among them, endopeptidases can be sub-classed as D,D-, L,D-, and D,L-endopeptidase referring to the stereochemistry of the cleaved amino acid residues. It is reasonably clear that PGHs play the key roles in the processes of (I) regulation of cell wall growth, (II) turnover of peptidoglycan, (III) separation of daughter cells, (□) liberation of spores from mother cells, (□) germination of spores to form vegetative cells, and (□) bacteria autolysis (Layec et al., 2008; Vollmer et al., 2008). Regulation of PGHs in these processes could affect pathogenic properties of some bacteria to their hosts. In Gram-positive bacteria, Amidases AtlA and SleI can affect bacterial biofilm formation, autolysis, and virulence in *Staphylococcus aureus* (Bose et al., 2012; Vermassen et al., 2019); lytic enzyme CbpD, LytA, LytB, and LytC can mediate lysis of non-competent target cells and cell separation in *Streptococcus pneumoniae* (Lopez et al., 2000; Eldholm et al., 2009). In Gram-negative strains, carboxypeptidase Pgp1 and Pgp2 of *Campylobacter jejuni* could reduce pathogenicity through impairing bacteria motility, biofilm formation, and bacteria colonization (Frirdich et al., 2012; Frirdich et al., 2014); N-acetylglucosaminidase (p60, FlaA) and N-acetylmuramoyl-L-alanine amidases (Ami, IspC) can affect cell separation, adhesion, virulence, and autolysis in *Listeria monocytogenes* (Wuenscher et al., 1993; Milohanic et al., 2001; Popowska and Markiewicz, 2004; Wang and Lin, 2008).

PGHs have been studied well in many pathogens, while the characterization and physiological functions of PGHs in *C. difficile* remains to be explored. In total, 37 PGHs belonging to each of the five hydrolase classes were predicted in *C. difficile*, among them are 13 endopeptidases, 10 N-acetylmuramoyl-L-alanine amidases, 8 carboxypeptidases, 3 N-acetylglucosaminidases, and 3 N-acetylmuramidases (Layec et al., 2008). Acd (N-acetylglucosaminidases, autolysin) which can hydrolyze peptidoglycan bonds between N-

acetylglucosamine and N-acetylmuramic acid identified by RP- HPLC and CwlT which contains a novel bacterial lysozyme domain and an NlpC/P60 D,L-endopeptidase domain as a bifunctional cell wall hydrolase were firstly identified in *C. difficile* 630, while the physiological functions of Acd and CwlT are still not clear (Dhalluin et al., 2005; Xu et al., 2014). Besides, SleC, a N-acetylglucosaminidases which is essential for *C. difficile* spore germination and SpoIIQ, an endopeptidase that is required for *C. difficile* spore formation have also been identified (Gutelius et al., 2014; Fimlaid et al., 2015). Recently, Cwp19, a novel lytic transglycosylase, which contributes to toxin release though bacteriolysis was reported in *C. difficile* 630 (Wydau-Dematteis et al., 2018).

Although several PGHs have been reported in *C. difficile*, more potential PGHs and their physiological functions need to be uncovered. In this study, we applied the Vaxign reverse vaccinology tool and characterized a new endopeptidase (CDR20291_0971, named as Cwl0971) *in vitro* and *in vivo*. Results showed that Cwl0971 is involved in cell wall lysis and cell viability, which affects several phenotypes of R20291. Our data indicate that the endopeptidase Cwl0971 is an attractive target for *C. difficile* infection therapeutics and prophylactics.

Results

Bioinformatic identification and analysis of putative cell wall hydrolase 0971

Vaxign is a web-based reverse vaccinology tool that uses comparative genomic sequence analysis to predict vaccine candidates based on different criteria such as cellular localization and adhesion probability (He et al., 2010). Using R20291 as the seed strain, Vaxign analysis predicted 31 *C. difficile* proteins to be cell membrane-bound, likely to be adhesins and hydrolases, and conserved in the other 12 *C. difficile* genomes. Among these proteins is YP_003217470.1, a putative cell wall hydrolase of 427 amino acids with a predicted molecular

weight of 44.82 kDa and a pI of 9.30. This new putative cell wall hydrolase (Cwl0971) classed into C40 family peptidase is encoded by the *CDR20291_ 0971* gene (shorted as 0971, NCBI Entrez Gene ID of 8468749) in strain R20291.

Based on the conserved domain analysis, Cwl0971 has a putative 27-amino acid signal sequence and two domains (Fig. 1A). The putative C-terminal catalytic domain belongs to the Spr (COG0791) and NlpC/P60 (pfam00877) superfamilies with endopeptidase activity. The N-terminal domain contains 3 bacterial SH3_3 domain which belongs to the YgiM superfamily (COG3103) predicted to act as the targeting domains involved in bacterial cell wall recognition and binding (Xu et al., 2015).

Construction of 0971 gene deletion mutant and analysis of growth profile and 0971 gene transcription

To analyze the function of the 0971 gene in R20291, CRISPR-AsCpfI based plasmid pDL1 (pMTL82151-Ptet-AscpfI) was constructed for gene deletion. Two sgRNAs targeting the 0971 gene in different loci were designed. A fragment of 422 bp of the 0971 gene was deleted with the pDL1-0971 plasmid, resulting in R20291Δ0971 mutant (Fig. 1 B). The correct deletion was verified with check primers 1-F/R and 2-F/R by PCR (Fig. 1 C). The 0971 gene complementation strain R20291Δ0971-pMTL84153/0971 (shorted as R20291Δ0971-C), and the control strain R20291-pMTL84153 and R20291Δ0971-pMTL84153 were constructed for 0971 function analysis.

The effect of the 0971 gene deletion on R20291 growth was evaluated in BHIS media. Our preliminary data showed that there was no significant difference in bacteria growth of R20291 VS R20291/pMTL84153 and R20291Δ0971 VS R20291Δ0971-pMTL84153 (data not shown). Therefore, we just compared R20291, R20291Δ0971, and R20291Δ0971-C. Fig. 1D showed that

there was no significant difference in bacteria growth between the wild type strain and mutant. The 0971 gene expression during *C. difficile* growth was determined by real-time quantitative PCR (RT-qPCR). As shown in Fig. 1E, transcription of the 0971 gene increased significantly at 24 h (*P < 0.05), 36 h (*P < 0.05), and 48 h post incubation (*P < 0.05). Interestingly, transcription of the 0971gene peaked at 24 h, followed by a slight decrease, and increased expression again at 48 h.

Effect of Cwl0971 defect on cell wall integrity

To determine if the Cwl0971 could affect *C. difficile* autolysis, the Triton X-100 autolysis assay was conducted. No significant difference in bacterial autolysis of R20291 VS R20291/pMTL84153 and R20291Δ0971 VS R20291Δ0971-pMTL84153 was detected (data not shown). As shown in Fig. 2A, R20291Δ0971 lysed at a slower rate than R20291 (*P < 0.05) indicating that the Cwl0971 defect increased bacterial resistance to Triton X-100 and impaired autolysis of R20291.

To check whether the cell wall of R20291Δ0971 was altered, we detected the LDH cytotoxicity of *C. difficile* strains. Fig. 2B showed that the permeability of R20291Δ0971 was lower than R20291 with a significant difference after 24 h of incubation (*P < 0.05), suggesting that the cell wall integrity of R20291Δ0971 might be changed. To further analyze the effect of the Cwl0971 defect on the cell, we analyzed *C. difficile* cell viability through live-dead cell staining. Four areas of cells (>400 cells) on a slide were counted with microscope software (dead bacteria were dyed as the red color with PI, and live bacteria were dyed as the green color with CFDA), and the percent of dead cells accounted in total cells were calculated (Fig. 2C). As shown in Fig. 2C and 2D, a significant reduction of dead cells of R20291Δ0971 were found at 36

h incubation (*P < 0.05). Taken together, our data confirmed that the cell autolysis of R20291Δ0971 decreased compared to R20291.

Purified Cwl0971 cleaves *Bacillus subtilis* cell wall

Cwl0971 was overexpressed as an N-terminal His-tagged fusion protein (without signal peptide) and purified with Ni^{2+} affinity chromatography column for zymogram analysis. As shown in Fig. 3A, clear reaction zones on the zymogram were detected suggesting that the Cwl0971 has a detectable cleavage activity for the *B. subtilis* cell wall. The correct protein band was also evidenced via Western blotting (Fig. 3B).

Effects of Cwl0971 defect on toxin expression

To evaluate the effect of 0971 gene deletion on toxin expression, the transcription of toxin genes (*tcdA* and *tcdB*) and the toxin concentration of culture supernatants at 12, 24, 36, and 48 h post inoculation were analyzed by RT-qPCR and ELISA. Our preliminary data showed that there was no significant difference in toxin expression of R20291 VS R20291/pMTL84153 and R20291Δ0971 VS R20291Δ0971-pMTL84153 (data not shown). Therefore, we just compared R20291, R20291Δ0971, and R20291Δ0971-C. As shown in Fig. 4A and 4B, no significant difference in toxin transcription of R20291 VS R20291Δ0971 was detected. Interestingly, Fig. 4C and 4D showed that the concentration of TcdA and TcdB of R20291Δ0971 was significantly lower than that of R20291 after 36 h post inoculation (*P □ 0.05). As shown in Fig. 4C, the TcdA concentration of R20291Δ0971 decreased by 26.5% (*P □ 0.05) at 36 h and 25.0% (*P □ 0.05) at 48 h. Fig. 4D showed that the TcdB concentration of R20291Δ0971 decreased by 15.1% (*P □ 0.05) at 36 h and 11.8% (*P □ 0.05) at 48 h. Our data suggested that Cwl0971 does not affect toxin transcription, but rather facilitate toxin release by altering the integrity of the cell wall and bacteriolysis.

Effects of Cwl0971 defect on sporulation, germination, and spores resistance to heat

To assay the sporulation ratio of *C. difficile* strains, R20291, R20291Δ0971, R20291Δ0971-C, R20291-pMTL84153, and R20291Δ0971-pMTL84153 were cultured in Clospore media for 120 h, respectively. As shown in Fig. 5A, the sporulation ratio of R20291Δ0971 decreased by 63.0% (***P* □ 0.01) compared to R20291 at 120 h post incubation. The germination ratio of *C. difficile* spores was evaluated as well. Fig. 5B showed that the 0971 gene deletion significantly impaired R20291 spores germination (**P* □ 0.05). The survival rate of spores to heat (65 □) was shown in Fig. 5C. R20291Δ0971 spores were more sensitive to heat compared to R20291 spores (**P* □ 0.05) and the heat sensitivity of R20291Δ0971 spores can be complemented by the 0971 complementation (data not shown).

Effects of Cwl0971 defect on biofilm formation, motility, and bacterial adhesion *in vitro*

To characterize the effects of 0971 gene deletion on *C. difficile* physiology, biofilm production of different *C. difficile* strains was first analyzed with RCM media. As shown in Fig. 5D, the biofilm production of R20291Δ0971 decreased by 40.3% (***$p < 0.001$) at 24 h and 20.5% (*$p < 0.05$) at 48 h compared to R20291. Following this, the motility (swimming and swarming) of wild type strain and mutant were analyzed on agar plates (Fig. S1), respectively. Fig. 5E showed that the diameter of the swarming halo of R20291Δ0971 increased 1.05 folds (****$p < 0.0001$) at 24 h post incubation and the swimming halo of R20291Δ0971 increased by 25.6% (**$p < 0.01$) at 12 h post incubation compared to R20291. The ability of *C. difficile* vegetative cells to adhere to HCT-8 cells *in vitro* was analyzed. Fig. 5F showed that the mean adhesion of R20291 was 2.40 ± 0.60 bacteria / cell, while R20291Δ0971 was 4.83 ± 0.52, which increased 1.01 folds (**P* □ 0.05) compared to R20291. The adhesion ability of complementation strains was recovered to the wild type level.

Evaluation of Cwl0971 defect on bacterial virulence in the CDI mouse model

To evaluate the effect of 0971 gene deletion on *C. difficile* virulence *in vivo*, the mouse model of CDI was used. Thirty mice (n=10 per group) were orally challenged with R20291 or R20291Δ0971 spores (1×10^6 spores / mouse) after antibiotic treatment. As shown in Fig. 6A, the R20291Δ0971 infection group lost less weight at days post challenge 3 (*P □ 0.05) compared to the R20291 infection group. Fig. 6B showed that only 20% of mice succumbed to severe disease within 4 days in the R20291Δ0971 infection group compared to 50% mortality in the R20291 infection group (no significant difference with log-rank analysis). Meanwhile, 100% of mice developed diarrhea in the R20291 infection group versus 80% in the R20291Δ0971 infection group at days post challenge 2 (Fig. 6C). As shown in Fig. 6D, the CFU of the R20291Δ0971 infection group decreased in the fecal shedding samples at days post challenge 1, 2, and 4 (*P □ 0.05) compared to the R20291 infection group.

To evaluate the toxin level in the gut, the titer of TcdA and TcdB in the feces was measured. In comparison with the R20291 infection group, the TcdA and TcdB of the R20291Δ0971 infection group decreased significantly at days post challenge 1 (*P □ 0.05), 2 (TcdA **P □ 0.01, TcdB ***P □ 0.001), 3 (*P □ 0.05), and 6 (*P □ 0.05) (Fig. 6E and 6F). Taken together, our results indicated that the Cwl0971 defect impaired R20291 pathogenicity.

Discussion

In this study, we reported the identification and characterization of a novel endopeptidase Cwl0971 from *C. difficile* R20291. Our data showed that Cwl0971 had a hydrolase activity for bacterial cell wall and it was involved in several cellular processes of *C. difficile* such as cell viability, biofilm formation, and bacteria motility. Notably, the depletion of Cwl0971 decreased sporulation, germination, cell autolysis which impaired toxin release, and decreased fitness over

the wild strain in the mouse infection model. Our results indicated that Cwl0971 could be a new potential antibacterial autolysin / target for small molecular inhibitors development for CDI therapeutics.

Cwl0971, a novel endopeptidase classified into C40 family peptidase, is composed of N-terminal 3 bacterial SH3_3 cell wall / substrate-binding domain and a C-terminal NlpC/P60 (pfam00877) domain with endopeptidase activity predicated through bioinformatics analysis with NCBI's Conserved Domain Database (CDD) (Fig. 1A). The C40 family peptidase/NlpC/P60 protein usually contains a conserved Cys-His-His catalytic triad that appears to be specific to murein tetrapeptide. It typically cleaves the linkage between D-Glu and L-diaminopimelic acid (L-DPA) (or Lys) within peptidoglycan stem peptides which was involved in cell wall hydrolysis during cell growth or cell lysis (Anantharaman and Aravind, 2003). The Cwl0971 NlpC/P60 domain structure was superimposed well with *E. coli* Spr protein which acts as γ-D-glutamyl-L-diaminopimelic acid endopeptidase through Ipred4 software prediction (http://www.compbio.dundee.ac.uk/jpred/) despite the low level of protein sequence identity (36% identity) between Cwl0971 and Spr (Aramini et al., 2008). SH3 (Src Homology 3) domains are protein interaction domains that bind proline-rich ligands with moderate affinity and selectivity, preferentially to PxxP motifs (Xu et al., 2015). Thus, they are referred to as proline-recognition domains (PRDs). SH3 domains containing proteins play versatile and diverse roles in the cell, including the regulation of enzymes, changing the subcellular localization of signaling pathway components, and mediating the formation of multiprotein complex assemblies (https://www.ncbi.nlm.nih.gov/Structure/cdd/cddsrv.cgi?ascbin=8&maxaln=10&seltype=2&uid=388381). To evaluate the roles of Cwl0971 in R20291, the 0971 gene was deleted successfully with CRISPR-AsCpfI plasmid (Fig. 1B and 1C). Meanwhile, the transcription of the 0971 gene

was determined by RT-qPCR (Fig. 1E). Results showed that the 0971 gene transcription increased at 24 h (*$P < 0.05$), 36 h (*$P < 0.05$), and 48 h (*$P < 0.05$) significantly compared to 12 h, and the transcription of the 0971 gene peaked at 24 h, followed a slight decrease, and increased again at 48 h, indicating that the 0971 gene plays important roles in both bacterial stationary and sporulation phases.

The bacterial cell wall has been reported to play crucial roles in bacterial physiology (Dmitriev et al., 2005). Peptidoglycan (PG), a dynamic macromolecule, is a primary cell wall constituent of Gram-positive bacteria and is constantly remodeled to enable bacterial growth and differentiation. Peptidoglycan hydrolases (PGHs) contribute to PG plasticity and play a key role in maintaining the cell wall shape through hydrolyzation of PG bonds. Among them, endopeptidase is one major peptidoglycan hydrolase involved in several cellular processes (Layec et al., 2008; Vollmer et al., 2008). Endopeptidase can be subclassified as D,D-endopeptidase, D,L-endopeptidase, and L,D-endopeptidase depending on their hydrolytic specificity. The D,D-endopeptidases hydrolase the D-Ala-DPA cross-bridges and can be classified into Type-4 and Type-7 PBPs (penicillin-binding protein) (Vollmer et al., 2008). Type-4 PBPs are generally indirectly involved in cell morphology, daughter cell separation, and biofilm formation, such as *E. coli* PBP4 and *B. subtilis* PBP4a (Duez et al., 2001; Harris et al., 2002; Vollmer et al., 2008). While type-7 PBPs are membrane-associated penicillin-sensitive D,D-endopeptidase with amphipathic helixes involved in non-growing *E. coli* lysis, such as *E. coli* PBP7 encoded by *pbpG* gene (Tuomanen and Schwartz, 1987; Henderson et al., 1995). The D,L-endopeptidases usually cleave the bond between D-Glu (position 2) and DPA (position 3) of the peptide and are classified as two different families based on Zn^{2+} dependence (Hourdou et al., 1992). CwlS, CwlO, LytE, and LytF from *B. sphaericus* and p60 from *L. monocytogenes* which

belong to the family II D,L-endopeptidases have been identified to regulate cell autolysis and division (Margot et al., 1998; Ohnishi et al., 1999; Pilgrim et al., 2003; Yamaguchi et al., 2004; Fukushima et al., 2006). YqgT, the Zn^{2+} dependent family I D,L-endopeptidases from *B. sphaericus*, was also studied (Hourdou et al., 1993). These L,D-endopeptidases cleave the bond between L-Ala (position 1) and D-Glu (position 2) in the stem peptide. CwlK is the first characterized L,D-endopeptidase in *B. subtilis*, which was expressed during the vegetative growth phase and probably localized in the membrane as a lipoprotein (Fukushima et al., 2007). LytH which expressed only during the sporulation phase in *B. subtilis* has been identified to be involved in spore cortex structure determination and maturation (Horsburgh et al., 2003). Recently, Cwp19 has been identified as a novel lytic transglycosylase that can catalyze muropeptide by using RP-HPLC associated with MALDI-TOF MS and MALDI-TOF/TOF tandem MS (MS/MS) (Wydau-Dematteis et al., 2018). The determination of catalytic specialty of endopeptidase Cwl0971 through RP-HPLC and MALDI-TOF/TOF tandem MS is underway in our group. While it is still not clear if Cwl0971 is D,D-, D,L- or L,D-endopeptidase, the effect of Cwl0971 depletion on *C. difficile* autolysis was demonstrated firstly. As shown in Fig. 2A, R20291Δ0971 lysed at a slower rate than R20291 did ($*P < 0.05$) in Triton X-100 induced cell autolysis assay, indicating that the depletion of Cwl0971 affects cell autolysis. Meanwhile, the cell permeability and cell viability of R20291Δ0971 were evaluated (Fig. 2B, 2 C, and 2D). The lower cell permeability and cell death of R20291Δ0971 detected ($*P < 0.05$) from the late stationary phase indicated that the Cwl0971 could affect cell viability through regulating cell wall structure and cell autolysis in *C. difficile*. To check the hydrolase activity of Cwl0971 *in vitro*, the Cwl0971 protein was purified and the hydrolytic activity was analyzed by zymography (Fig. 3A and 3B). The clear reaction zones on the zymogram were detected, strongly indicating

the hydrolytic activity of Cwl0971 *in vitro*. Taken together, our data clearly showed the Cwl0971 is a novel cell wall hydrolase (endopeptidase) that is involved in *C. difficile* autolysis.

Two exotoxins (TcdA and TcdB) have been identified as the major virulence factors of *C. difficile (Kuehne et al., 2010)*. Several genes, such as *tcdC*, *tcdE*, and *tcdR*, are involved in the regulation of toxin gene expression (Mani et al., 2002; Dupuy et al., 2008; Govind and Dupuy, 2012; Govind et al., 2015). TcdA and TcdB are the large clostridial glucosylation family toxins that are secreted without signal peptide (Popoff and Bouvet, 2009). Except for reported regulation genes, toxin release is also associated with *C. difficile* cell autolysis. Wydau-Dematteis et al. (Wydau-Dematteis et al., 2018) identified that Cwp19 contributes to toxin release through bacteriolysis, which indicated that TcdE and bacteriolysis were the coexisting mechanisms for toxin release. Cwp22, a novel peptidoglycan cross-linking enzyme, was reported to be involved in *C. difficile* cell wall integrity and toxin release in our previous study (Zhu et al., 2019). In this study, our data showed that the concentration of TcdA and TcdB in mutant supernatants both decreased ($*p < 0.05$) after 36 h post inoculation (Fig. 4C and 4D), while the transcription of toxin genes was not affected by 0971 gene deletion (Fig. 4A and 4B). These results indicated that Cwl0971 can affect toxin release through bacteriolysis.

PGHs have been identified to be involved in several cellular processes (Layec et al., 2008; Vollmer et al., 2008). Haiser et al. (Haiser et al., 2009) demonstrated that cell wall hydrolase RpfA, SwlA, SwlB, and SwlC play critical roles at multiple stages in *Streptomyces coelicolor* growth and development. The deletion of each of these four hydrolase genes could impair bacteria heat resistance, vegetative growth, spore formation, and spore germination. Of the 37 PGHs predicted in *C. difficile* 630, Acd (autolysin), CwlT (bifunctional cell wall hydrolase with lysozyme and D,L-endopeptidase activities), SpoIIQ (endopeptidase), and SleC (N-

acetylglucosaminidases) have been studied (Dhalluin et al., 2005; Layec et al., 2008; Gutelius et al., 2014; Xu et al., 2014; Fimlaid et al., 2015). But the physiological functions of Acd and CwlT in *C. difficile* are still unclear. Fimlaid et al. (Fimlaid et al., 2015) found that the depletion of SpoIIQ which has been identified as a Zn^{2+} dependent M23 peptidase in *C. difficile* could impair engulfment, tethering of coat to the forespore, and heat-resistant spore formation. Gutelius et al. (Gutelius et al., 2014) characterized the lytic transglycosylase SleC which is essential for *C. difficile* spore germination. *C. difficile* spore formation allows bacteria to survive in harsh environmental conditions, such as oxygen-rich environments, disinfectants, heat, and gastrointestinal tract (Haiser et al., 2009; Gil et al., 2017). In order to cause disease, *C. difficile* spores must germinate into the vegetative cells. Thus sporulation and germination of *C. difficile* play the key roles in *C. difficile* pathogenesis, transmission, and persistence of CDI (Zhu et al., 2018). These reported studies prompted us to examine the effects of the 0971 gene deletion on some other *C. difficile* phenotypes, such as sporulation, germination, spore heat-resistance, motility, biofilm formation, and adhesion (Fig. 5). Our data showed that Cwl0971 mutant exhibited defects in sporulation (Fig. 5A, decreased by 63.0%, $^{**}p < 0.01$), spore germination (Fig. 5B, $^{*}p < 0.05$), and spore heat-resistance (Fig. 5C, $^{*}p < 0.05$). The defects of sporulation and germination in R20291Δ0971 contribute to the decreased pathogenicity of *C. difficile*. Our data (Fig. 5D) showed that the biofilm production of R20291Δ0971 decreased by 40.3% ($^{***}p < 0.001$) at 24 h and 20.5% ($^{*}p < 0.05$) at 48 h compared to R20291. Biofilms contribute to survival, persistence, antimicrobial resistance, colonization, and disease for many pathogens and it has been reported that up to 80% of bacterial infections were linked to biofilms (Flemming and Wingender, 2010). In *C. difficile*, the master regulator of sporulation (Spo0A) and cell wall protein (Cwp84) have been reported to be involved in biofilm formation (Dawson et al., 2012;

Ethapa et al., 2013). The decrease of biofilm production in *C. difficile* Spo0A and Cwp84 mutants indicated the possible link between sporulation and biofilm formation and other CWPs may be also involved in biofilm formation (Dawson et al., 2012; Dapa and Unnikrishnan, 2013; Ethapa et al., 2013). We detected the transcription of *spo0A* in R20291Δ0971 (data not shown), results showed that the expression of *spo0A* gene decreased significantly (*$p < 0.05$) which was also consistent with our sporulation analysis (Fig. 5A). As shown in Fig. 5E and 5F, R20291Δ0971 showed increased motility (swarming increased 1.05 folds, ****$p < 0.0001$ and swimming increased by 25.6%, **$p < 0.01$) and adherence (increased 1.01 folds, *P □ 0.05) with significant difference compared to R20291. El Meouche et al. (El Meouche et al., 2013) reported that SigD is implicated in the positive regulation of *C. difficile* motility. We detected the transcription of *sigD* gene in our study (data not shown), and results showed that there was no significant difference in *sigD* expression (*$P > 0.05$) between R20291Δ0971 and R20291. Previous studies have highlighted that the flagella (motility) of *C. difficile* play an important role in biofilm formation and bacteria adherence to host (Tasteyre et al., 2001), but the results from different groups are controversial. In *C. difficile* 630Δerm, previous reports have shown that the *fliC* mutation (motility defect) could enhance toxin production and bacteria adherence to the host (Dingle et al., 2011; Aubry et al., 2012; Baban et al., 2013). While in R20291, the *fliC* mutation decreased biofilm formation and adherence to Caco-2 cells (Baban et al., 2013; Ethapa et al., 2013). The complex relationship between biofilm formation, motility, and adhesin requires further study to fully understand their coordinated mechanism. Collectively, the data presented in this study suggested that Cwl0971 defect impairs the pleiotropic cellular processes in *C. difficile* which resulted in decreased pathogenicity in mouse CDI model (Fig. 6).

In conclusion, we characterized the cell wall hydrolase Cwl0971 and demonstrated the pleiotropic crucial roles of Cwl0971 in R20291. Cwl0971 is an attractive antibacterial autolysin and a potential important target for small molecular inhibitors development for CDI therapeutics.

Experimental procedures

Comparative genomic analysis of *C. difficile* genomes

Using the Vaxign reverse vaccinology tool (He et al., 2010), we systematically analyzed all proteins in the genome of *C. difficile* strain R20291 in terms of cellular localization, adhesin probability, transmembrane helices, sequence conversation with the genomes of other 12 *C. difficile* strains, sequence similarity to human and mouse proteins and protein length. These other 12 strains are strains 630, BI1, ATCC 43255, CD196, CIP 107932, QCD-23m63, QCD-32g58, QCD-37x79, QCD-63q42, QCD-66c26, QCD-76w55, and QCD-97b34. Protein-conserved domain analysis was performed using the NCBI's CDD.

Bacteria, plasmids, and culture conditions

Table 1 lists the strains and plasmids used in this study. *C. difficile* strains were cultured in BHIS (brain heart infusion broth supplemented with 0.5% yeast extract and 0.1% L-cysteine, and 1.5% agar for agar plates) at 37 □ in an anaerobic chamber (90% N_2, 5% H_2, 5% CO_2). For spores preparation, *C. difficile* strains were cultured in Clospore media and purified as described (Perez et al., 2011). *Escherichia coli* DH5α, *E. coli* HB101/pRK24, and *E. coli* BL21 (DE3) were grown aerobically at 37 □ in LB media (1% tryptone, 0.5% yeast extract, 1% NaCl). Among them, *E. coli* DH5α was used as a cloning host, *E. coli* HB101/pRK24 was used as a conjugation donor host, and *E. coli* BL21 (DE3) was used as a protein expression host. Antibiotics were added when needed: for *E. coli*, 15 μg ml^{-1} chloramphenicol, 50 μg ml^{-1} kanamycin; for *C.*

411 *difficile*, 15 μg ml^{-1} thiamphenicol, 250 μg ml^{-1} D-cycloserine, 50 μg ml^{-1} kanamycin, 8 μg ml^{-1}
412 cefoxitin, and 500 ng ml^{-1} anhydrotetracycline.

413 **DNA manipulations and chemicals**

414 DNA manipulations were carried out according to standard techniques (Chong, 2001). Plasmids
415 were conjugated into *C. difficile* as described earlier (Heap et al., 2010). The DNA markers,
416 protein markers, PCR product purification kit, DNA gel extraction kit, restriction enzymes,
417 cDNA synthesis kit, and SYBR Green RT-qPCR kit were purchased from Thermo Fisher
418 Scientific (Waltham, USA). PCRs were performed with the high-fidelity DNA polymerase NEB
419 Q5 Master Mix, and PCR products were assembled into target plasmids with NEBuilder HIFI
420 DNA Assembly Master Mix (New England, UK). Primers (Supporting Information Table S1)
421 were purchased from IDT (Coralville, USA). All chemicals were purchased from Sigma (St.
422 louis, USA) unless those stated otherwise.

423 **Construction of 0971 deletion mutant and complementation strains**

424 The Cas12a (AsCpfI) based gene deletion plasmid pDL-1 was constructed and used for *C.*
425 *difficile* gene deletion (Hong et al., 2018). Target sgRNAs were designed with an available
426 website tool (http://big.hanyang.ac.kr/cindel/), and the off-target prediction was analyzed on the
427 Cas-OFFinder website (http://www.rgenome.net/cas-offinder/). The sgRNA and homologous
428 arms (up and down) were assembled into pDL-1. Two sgRNAs targeting the 0971 gene were
429 designed and used for gene deletion plasmid construction in *C. difficile*. Briefly, the gene
430 deletion plasmid was constructed in the cloning host *E. coli* DH5α and was transformed into the
431 donor host *E. coli* HB101/pRK24, and subsequently was conjugated into R20291. Potential
432 successful transconjugants were selected with selective antibiotic BHIS-TKC plates (15 μg ml^{-1}
433 thiamphenicol, 50 μg ml^{-1} kanamycin, 8 μg ml^{-1} cefoxitin). The transconjugants were cultured in

BHIS-Tm broth (15 μg ml^{-1} thiamphenicol) to log phase, then the subsequent cultures were plated on induction plates (BHIS-Tm-ATc: 15 μg ml^{-1} thiamphenicol and 500 ng ml^{-1} anhydrotetracycline). After 24 - 48 h incubation, 20 - 40 colonies were selected and used as templates for colony PCR test with check primers 1-F/R and 2-F/R. The correct gene deletion colony was subcultured into BHIS broth without antibiotics and was passaged several times for plasmid cure to get a clean gene deletion mutant R20291Δ0971. The R20291Δ0971 genome was isolated and used as the template for PCR test with 1-F/R and 2-F/R primers, and the PCR products were sequenced to confirm the correct gene deletion.

The 0971 gene was amplified with primer 3-F/R and assembled into *Sac*I-*Bam*HI digested pMTL84153 plasmid, yielding the complementation plasmid pMTL84153-0971, and was subsequently conjugated into R20291Δ0971, yielding R20291Δ0971/pMTL84153-0971 (shorted as R20291Δ0971-C). The blank plasmid pMTL84153 was also conjugated into R20291 and R20291Δ0971 as negative controls, respectively.

Growth profile, cell autolysis, LDH cytotoxicity, and cell viability assay

C. difficile strains were incubated to an optical density of OD_{600} of 0.8 in BHIS and were diluted to an OD_{600} of 0.2. Then, 1% of the culture was inoculated into fresh BHIS, followed by measuring OD_{600} for 34 h.

To determine Triton X-100 induced autolysis, *C. difficile* strains were cultured to an OD_{600} of 0.8 to log phase, and then 5 ml of each culture was collected and washed with 50 mM potassium phosphate buffer (pH 7.0). The pellets were resuspended in a final volume of 2.5 ml of 50 mM potassium phosphate buffer with or without 0.1% of Triton X-100. Afterward, the bacteria were incubated anaerobically at 37 °C, and the OD_{600} was detected once every 10 min for 120 min. The lysis percent was shown as % initial OD_{600}.

For LDH cytotoxicity analysis, the supernatants from different strains were collected and filtered with 0.22 μm filters, then the LDH concentration of the supernatants was detected with the Pierce™ LDH Cytotoxicity Assay Kit (Thermo Fisher, USA) according to the instructions of the manufacturer.

For cell viability analysis, the live-dead cell staining was performed (Zhu et al., 2019). Briefly, 12 and 36 h post incubated *C. difficile* strains were collected and cell number was normalized to 10^8 CFU/ml, respectively. Then 1 ml of each strain cultures were centrifuged at 4 □, 5000×*g* for 10 min, and washed 3 times with PBS. Afterward, the bacteria were resuspended in 100 μl of 0.1 mM sodium phosphonate buffer. The chemical 5(6)-CFDA (5-(and -6)-Carboxyfluorescein diacetate) was used to dye live *C. difficile*, and the propidium iodide (PI) was used to dye dead bacteria. The final concentration of 50 mM 5(6)-CFDA and 200 ng ml^{-1} of PI were used to co-dye *C. difficile* strains. *C. difficile* cells were incubated at 4 □ overnight for monitoring under a fluorescence microscope. The CFDA and PI were excited at 495 nm and 538 nm, respectively.

Purification and hydrolase activity assay of Cwl0971

The 0971 gene encoding the predicted binding and catalytic domains (without signal peptide) was PCR amplified with primer 4-F/R and assembled into *Nco*I-*Xho*I digested pET28a expression plasmid. 6×His tag was fused into the N-terminal of Cwl0971 for protein purification with Ni^{2+} affinity chromatography column. The protein was purified as described earlier (Peng et al., 2018).

The hydrolytic activity of purified Cwl0971 was evaluated with a zymogram assay (Leclerc and Asselin, 1989). Briefly, cell wall material (0.1%, wt/vol, 200 μl of a 50 mg ml^{-1} autoclaved *Bacillus subtilis* cell suspension was added) was incorporated into SDS polyacrylamide

separating gels. Following constant voltage electrophoresis (100 V) at 4 □, gels were washed 3 times with water for 10 minutes at room temperature, then transferred to a renaturing buffer (20 mM Tris, 50 mM NaCl, 20 mM $MgCl_2$, 0.5% Triton X-100, pH 7.4) and washed gently overnight at 37 □. The renatured Cwl0971 appeared as slightly clear bands on an opaque background. The contrast was enhanced by staining the gels with 0.1% (wt/vol) methylene blue, 0.01% (wt/vol) KOH for 2 h. Zymogram was run in parallel with Western blot detection gels to confirm that the proteins migrated at the correct size.

Toxin expression assay

To evaluate the toxin expression in *C. difficile* strains, 10 ml of *C. difficile* cultures were collected at 12, 24, 36, and 48 h post incubation. The cultures were adjusted to the same density with fresh BHIS. Then the cultures were centrifuged at 4 □, 8000×*g* for 15 min, filtered with 0.22 μm filters and used for ELISA. Anti-TcdA (PCG4.1, Novus Biologicals, USA) and anti-TcdB (AI, Gene Tex, USA) were used as coating antibodies for ELISA, and HRP-Chicken anti-TcdA and HRP-Chicken anti-TcdB (Gallus Immunotech, USA) were used as detection antibodies.

For toxin transcription analysis, 2 ml of 12, 24, 36, and 48 h post inoculated *C. difficile* cultures were centrifuged at 4 □, 12000×*g* for 5 min, respectively. Then, the total RNA of different strains was extracted with TRIzol reagent. The transcription of *tcdA* and *tcdB* was measured by RT-qPCR with Q-*tcdA*-F/R and Q-*tcdB*-F/R primers, respectively. All RT-qPCRs were repeated in triplicate, independently. Data were analyzed by using the comparative CT ($2^{-\Delta\Delta CT}$) method with 16s rRNA as a control.

Sporulation, germination, and spore resistance assay

C. difficile germination and sporulation analysis were conducted as reported earlier (Zhu et al., 2019). Briefly, for *C. difficile* sporulation analysis, *C. difficile* strains were cultured in Clospore media for 5 days, and the CFU of cultures were counted on BHIS plates with or without 0.1% TA to detect sporulation ratio, respectively. The sporulation ratio was calculated as CFU (65 □ heated) / CFU (no heated). For *C. difficile* germination assay, *C. difficile* spores were collected from 2-week Clospore media cultured bacteria and purified with sucrose gradient layer (50%, 45%, 35%, 25%, 10%). The heated purified spores were diluted to an OD_{600} of 1.0 in the germination buffer [10 mM Tris (pH 7.5), 150 mM NaCl, 100 mM glycine, 10 mM taurocholic acid (TA)] to detect the germination ratio. The value of OD_{600} was monitored immediately (0 min, t_0) and detected once every 2 min (t_x) for 20 min at 37 □. The germination ratio was calculated as OD_{600} (tx) / OD_{600} (T_0). Spores in germination buffer without TA were used as a negative control. To evaluate the spore resistance to heat, the sucrose gradient-purified *C. difficile* spores were shocked in a 65 □ water bath for 1 - 4 h. Afterward, the spores were plated on BHIS plates with 0.1% TA. The survival rate was calculated as CFU (65 □ heated) / CFU (no heated).

Biofilm and motility assay

For biofilm analysis, *C. difficile* strains were cultured to an OD_{600} of 0.8, and 1% of *C. difficile* cultures were inoculated into Reinforced Clostridial Medium (RCM) with 8 well repeats in 96-well plate and incubated in the anaerobic chamber at 37 □ for 24 and 48 h. The formation of biofilm was analyzed by crystal violet dye. Briefly, *C. difficile* cultures were removed by pipette carefully. Then 100 µl of 2.5% glutaraldehyde was added into the well to fix the bottom biofilm, and the plate was kept at room temperature for 30 min. Next, the wells were washed 3 times with PBS and dyed with 0.25% (w/v) crystal violet for 10 min. The crystal violet solution was

525 removed, and the wells were washed 5 times with PBS, followed by the addition of acetone into
526 wells to dissolve the crystal violet of the cells. The dissolved solution was further diluted with
527 ethanol 2 - 4 times and then detected at OD_{570}.

528 To examine the effect of 0971 gene deletion on *C. difficile* motility, *C. difficile* strains were
529 cultured to an OD_{600} of 0.8. For swimming analysis, 2 µl of *C. difficile* culture was penetrated
530 into soft BHIS agar (0.175%) plates, meanwhile, 2 µl of culture was dropped onto 0.3% BHIS
531 agar plates for swarming analysis. The swimming assay plates were incubated for 12 h and the
532 swarming plates were incubated for 24 h, respectively.

533 **Adhesion of *C. difficile* vegetative cells to HCT-8 cells**

534 *C. difficile* adhesion ability was evaluated with HCT-8 cells (ATCC CCL-244) (Janvilisri et al.,
535 2010). Briefly, HCT-8 cells were grown to 95% confluence (2×10^5/well) in a 24-well plate and
536 then moved into the anaerobic chamber, followed by infecting with 6×10^6 of log phase of *C.*
537 *difficile* vegetative cells at a multiplicity of infection (MOI) of 30:1. The plate was cultured at 37 □
538 for 30 min. After incubation, the infected cells were washed with 300 µl of PBS 3 times, and
539 then suspended in RPMI media with trypsin and plated on BHIS agar plates to enumerate the
540 adhered *C. difficile* cells. The adhesion ability of *C. difficile* to HCT-8 cells was calculated as
541 follow: CFU of adhered bacteria / total cell numbers.

542 **Evaluation of virulence of R20291 and R20291Δ0971 in the mouse model of *C. difficile***
543 **infection**

544 C57BL/6 female mice (6 weeks old) were ordered from Charles River Laboratories, Cambridge,
545 MA. All studies were approved by the Institutional Animal Care and Use Committee of
546 University of South Florida. The experimental design and antibiotic administration were
547 conducted as previously described (Sun et al., 2011). Briefly, 20 mice were divided into 2 groups

548 in 4 cages. Group 1 mice were challenged with R20291 spores and group 2 mice with
549 R20291Δ0971 spores, respectively. Mice were given an orally administered antibiotic cocktail
550 (kanamycin 0.4 mg ml^{-1}, gentamicin 0.035 mg ml^{-1}, colistin 0.042 mg ml^{-1}, metronidazole 0.215
551 mg ml^{-1}, and vancomycin 0.045 mg ml^{-1}) in drinking water for 4 days. After 4 days of antibiotic
552 treatment, all mice were given autoclaved water for 2 days, followed by one dose of clindamycin
553 (10 mg kg^{-1}, intraperitoneal route) 24 h before spores challenge (Day 0). After that, mice were
554 orally gavaged with 10^6 of spores and monitored daily for a week for changes in weight, diarrhea,
555 mortality, and other symptoms of the disease.

556 **Determination of *C. difficile* spores and toxin levels in feces**

557 Fecal pellets from post infection day 0 to day 7 were collected and stored at -80 □. To enumerate
558 *C. difficile* numbers, feces were diluted with PBS at a final concentration of 0.1 g ml^{-1}, followed
559 by adding 900 µl of absolute ethanol into 100 µl of the fecal solution, and kept at room
560 temperature for 1 h to inactivate vegetative cells. Afterward, fecal samples were serially diluted
561 and plated on BHIS-CCT plates (250 µg ml^{-1} D-cycloserine, 8 µg ml^{-1} cefoxitin, 0.1% TA). After
562 48 h incubation, colonies were counted and expressed as CFU/g feces. To evaluate toxin tilter in
563 feces, 0.1 g ml^{-1} of the fecal solution was diluted two times with PBS, followed by examining
564 TcdA and TcdB ELISA test.

565 **Statistical analysis**

566 The reported experiments were conducted in independent biological triplicates with the
567 exception of animal experiments, and each sample was additionally taken in technical triplicates.
568 Animal survivals were analyzed by Kaplan-Meier survival analysis and compared by the Log-
569 Rank test. Student's unpaired *t*-test was used for two groups comparison. One-way analysis of
570 variance (ANOVA) was used for more than two groups comparison. Results were expressed as

mean ± standard error of the mean. Differences were considered statistically significant if $P < 0.05$ (*).

Acknowledgments

This work was supported in part by the National Institutes of Health grants (K01-DK092352, R21-AI113470, R03-DK112004, and R01-AI132711 to X. Sun and AI124458 to L. N. Shaw).

Conflict of interest

The authors declare that they have no conflict of interest.

References

Anantharaman, V., and Aravind, L. (2003) Evolutionary history, structural features and biochemical diversity of the NlpC/P60 superfamily of enzymes. *Genome Biol* **4**: R11.

Aramini, J.M., Rossi, P., Huang, Y.J., Zhao, L., Jiang, M., Maglaqui, M. et al. (2008) Solution NMR structure of the NlpC/P60 domain of lipoprotein Spr from Escherichia coli: structural evidence for a novel cysteine peptidase catalytic triad. *Biochemistry* **47**: 9715-9717.

Aubry, A., Hussack, G., Chen, W., KuoLee, R., Twine, S.M., Fulton, K.M. et al. (2012) Modulation of toxin production by the flagellar regulon in Clostridium difficile. *Infect Immun* **80**: 3521-3532.

Baban, S.T., Kuehne, S.A., Barketi-Klai, A., Cartman, S.T., Kelly, M.L., Hardie, K.R. et al. (2013) The role of flagella in Clostridium difficile pathogenesis: comparison between a non-epidemic and an epidemic strain. *PLoS One* **8**: e73026.

Borriello, S.P., Davies, H.A., Kamiya, S., Reed, P.J., and Seddon, S. (1990) Virulence factors of Clostridium difficile. *Rev Infect Dis* **12 Suppl 2**: S185-191.

Bose, J.L., Lehman, M.K., Fey, P.D., and Bayles, K.W. (2012) Contribution of the Staphylococcus aureus Atl AM and GL murein hydrolase activities in cell division, autolysis, and biofilm formation. *PLoS One* **7**: e42244.

Braun, V., Hundsberger, T., Leukel, P., Sauerborn, M., and von Eichel-Streiber, C. (1996) Definition of the single integration site of the pathogenicity locus in Clostridium difficile. *Gene* **181**: 29-38.

Chong, L. (2001) Molecular cloning - A laboratory manual, 3rd edition. *Science* **292**: 446-446.

Dapa, T., and Unnikrishnan, M. (2013) Biofilm formation by Clostridium difficile. *Gut Microbes* **4**: 397-402.

Dawson, L.F., Valiente, E., Faulds-Pain, A., Donahue, E.H., and Wren, B.W. (2012) Characterisation of Clostridium difficile biofilm formation, a role for Spo0A. *PLoS One* **7**: e50527.

606 Dhalluin, A., Bourgeois, I., Pestel-Caron, M., Camiade, E., Raux, G., Courtin, P. et al. (2005)
607 Acd, a peptidoglycan hydrolase of Clostridium difficile with N-acetylglucosaminidase activity.
608 *Microbiology* **151**: 2343-2351.
609 Dingle, T.C., Mulvey, G.L., and Armstrong, G.D. (2011) Mutagenic analysis of the Clostridium
610 difficile flagellar proteins, FliC and FliD, and their contribution to virulence in hamsters. *Infect*
611 *Immun* **79**: 4061-4067.
612 Dmitriev, B., Toukach, F., and Ehlers, S. (2005) Towards a comprehensive view of the bacterial
613 cell wall. *Trends Microbiol* **13**: 569-574.
614 Dubberke, E.R., and Olsen, M.A. (2012) Burden of Clostridium difficile on the healthcare
615 system. *Clin Infect Dis* **55 Suppl 2**: S88-92.
616 Duez, C., Vanhove, M., Gallet, X., Bouillenne, F., Docquier, J., Brans, A., and Frere, J. (2001)
617 Purification and characterization of PBP4a, a new low-molecular-weight penicillin-binding
618 protein from Bacillus subtilis. *J Bacteriol* **183**: 1595-1599.
619 Dupuy, B., Govind, R., Antunes, A., and Matamouros, S. (2008) Clostridium difficile toxin
620 synthesis is negatively regulated by TcdC. *J Med Microbiol* **57**: 685-689.
621 El Meouche, I., Peltier, J., Monot, M., Soutourina, O., Pestel-Caron, M., Dupuy, B., and Pons,
622 J.L. (2013) Characterization of the SigD regulon of C. difficile and its positive control of toxin
623 production through the regulation of tcdR. *PLoS One* **8**: e83748.
624 Eldholm, V., Johnsborg, O., Haugen, K., Ohnstad, H.S., and Havarstein, L.S. (2009) Fratricide in
625 Streptococcus pneumoniae: contributions and role of the cell wall hydrolases CbpD, LytA and
626 LytC. *Microbiology* **155**: 2223-2234.
627 Ethapa, T., Leuzzi, R., Ng, Y.K., Baban, S.T., Adamo, R., Kuehne, S.A. et al. (2013) Multiple
628 factors modulate biofilm formation by the anaerobic pathogen Clostridium difficile. *J Bacteriol*
629 **195**: 545-555.
630 Fimlaid, K.A., Jensen, O., Donnelly, M.L., Siegrist, M.S., and Shen, A. (2015) Regulation of
631 Clostridium difficile Spore Formation by the SpoIIQ and SpoIIIA Proteins. *PLoS Genet* **11**:
632 e1005562.
633 Flemming, H.C., and Wingender, J. (2010) The biofilm matrix. *Nat Rev Microbiol* **8**: 623-633.
634 Frirdich, E., Biboy, J., Adams, C., Lee, J., Ellermeier, J., Gielda, L.D. et al. (2012)
635 Peptidoglycan-modifying enzyme Pgp1 is required for helical cell shape and pathogenicity traits
636 in Campylobacter jejuni. *PLoS Pathog* **8**: e1002602.
637 Frirdich, E., Vermeulen, J., Biboy, J., Soares, F., Taveirne, M.E., Johnson, J.G. et al. (2014)
638 Peptidoglycan LD-carboxypeptidase Pgp2 influences Campylobacter jejuni helical cell shape
639 and pathogenic properties and provides the substrate for the DL-carboxypeptidase Pgp1. *J Biol*
640 *Chem* **289**: 8007-8018.
641 Fukushima, T., Yao, Y., Kitajima, T., Yamamoto, H., and Sekiguchi, J. (2007) Characterization
642 of new L,D-endopeptidase gene product CwlK (previous YcdD) that hydrolyzes peptidoglycan
643 in Bacillus subtilis. *Mol Genet Genomics* **278**: 371-383.
644 Fukushima, T., Afkham, A., Kurosawa, S., Tanabe, T., Yamamoto, H., and Sekiguchi, J. (2006)
645 A new D,L-endopeptidase gene product, YojL (renamed CwlS), plays a role in cell separation
646 with LytE and LytF in Bacillus subtilis. *J Bacteriol* **188**: 5541-5550.
647 Gil, F., Lagos-Moraga, S., Calderon-Romero, P., Pizarro-Guajardo, M., and Paredes-Sabja, D.
648 (2017) Updates on Clostridium difficile spore biology. *Anaerobe* **45**: 3-9.
649 Govind, R., and Dupuy, B. (2012) Secretion of Clostridium difficile toxins A and B requires the
650 holin-like protein TcdE. *PLoS Pathog* **8**: e1002727.

651 Govind, R., Fitzwater, L., and Nichols, R. (2015) Observations on the Role of TcdE Isoforms in
652 Clostridium difficile Toxin Secretion. *J Bacteriol* **197**: 2600-2609.
653 Gutelius, D., Hokeness, K., Logan, S.M., and Reid, C.W. (2014) Functional analysis of SleC
654 from Clostridium difficile: an essential lytic transglycosylase involved in spore germination.
655 *Microbiology* **160**: 209-216.
656 Haiser, H.J., Yousef, M.R., and Elliot, M.A. (2009) Cell wall hydrolases affect germination,
657 vegetative growth, and sporulation in Streptomyces coelicolor. *J Bacteriol* **191**: 6501-6512.
658 Harris, F., Brandenburg, K., Seydel, U., and Phoenix, D. (2002) Investigations into the
659 mechanisms used by the C-terminal anchors of Escherichia coli penicillin-binding proteins 4, 5,
660 6 and 6b for membrane interaction. *Eur J Biochem* **269**: 5821-5829.
661 He, Y., Xiang, Z., and Mobley, H.L. (2010) Vaxign: the first web-based vaccine design program
662 for reverse vaccinology and applications for vaccine development. *J Biomed Biotechnol* **2010**:
663 297505.
664 Heap, J.T., Kuehne, S.A., Ehsaan, M., Cartman, S.T., Cooksley, C.M., Scott, J.C., and Minton,
665 N.P. (2010) The ClosTron: Mutagenesis in Clostridium refined and streamlined. *J Microbiol*
666 *Methods* **80**: 49-55.
667 Henderson, T.A., Templin, M., and Young, K.D. (1995) Identification and cloning of the gene
668 encoding penicillin-binding protein 7 of Escherichia coli. *J Bacteriol* **177**: 2074-2079.
669 Hong, W., Zhang, J., Cui, G., Wang, L., and Wang, Y. (2018) Multiplexed CRISPR-Cpf1-
670 Mediated Genome Editing in Clostridium difficile toward the Understanding of Pathogenesis of
671 C. difficile Infection. *ACS Synth Biol* **7**: 1588-1600.
672 Horsburgh, G.J., Atrih, A., and Foster, S.J. (2003) Characterization of LytH, a differentiation-
673 associated peptidoglycan hydrolase of Bacillus subtilis involved in endospore cortex maturation.
674 *J Bacteriol* **185**: 3813-3820.
675 Hourdou, M.L., Duez, C., Joris, B., Vacheron, M.J., Guinand, M., Michel, G., and Ghuysen, J.M.
676 (1992) Cloning and nucleotide sequence of the gene encoding the gamma-D-glutamyl-L-diamino
677 acid endopeptidase II of Bacillus sphaericus. *FEMS Microbiol Lett* **70**: 165-170.
678 Hourdou, M.L., Guinand, M., Vacheron, M.J., Michel, G., Denoroy, L., Duez, C. et al. (1993)
679 Characterization of the sporulation-related gamma-D-glutamyl-(L)meso-diaminopimelic-acid-
680 hydrolysing peptidase I of Bacillus sphaericus NCTC 9602 as a member of the metallo(zinc)
681 carboxypeptidase A family. Modular design of the protein. *Biochem J* **292 (Pt 2)**: 563-570.
682 Janoir, C. (2016) Virulence factors of Clostridium difficile and their role during infection.
683 *Anaerobe* **37**: 13-24.
684 Janvilisri, T., Scaria, J., and Chang, Y.F. (2010) Transcriptional profiling of Clostridium difficile
685 and Caco-2 cells during infection. *J Infect Dis* **202**: 282-290.
686 Kuehne, S.A., Cartman, S.T., Heap, J.T., Kelly, M.L., Cockayne, A., and Minton, N.P. (2010)
687 The role of toxin A and toxin B in Clostridium difficile infection. *Nature* **467**: 711-713.
688 Layec, S., Decaris, B., and Leblond-Bourget, N. (2008) Diversity of Firmicutes peptidoglycan
689 hydrolases and specificities of those involved in daughter cell separation. *Res Microbiol* **159**:
690 507-515.
691 Leclerc, D., and Asselin, A. (1989) Detection of bacterial cell wall hydrolases after denaturing
692 polyacrylamide gel electrophoresis. *Can J Microbiol* **35**: 749-753.
693 Lessa, F.C., Gould, C.V., and McDonald, L.C. (2012) Current status of Clostridium difficile
694 infection epidemiology. *Clin Infect Dis* **55 Suppl 2**: S65-70.
695 Lessa, F.C., Mu, Y., Bamberg, W.M., Beldavs, Z.G., Dumyati, G.K., Dunn, J.R. et al. (2015)
696 Burden of Clostridium difficile infection in the United States. *N Engl J Med* **372**: 825-834.

Lopez, R., Gonzalez, M.P., Garcia, E., Garcia, J.L., and Garcia, P. (2000) Biological roles of two new murein hydrolases of Streptococcus pneumoniae representing examples of module shuffling. *Res Microbiol* **151**: 437-443.

Mani, N., and Dupuy, B. (2001) Regulation of toxin synthesis in Clostridium difficile by an alternative RNA polymerase sigma factor. *Proc Natl Acad Sci U S A* **98**: 5844-5849.

Mani, N., Lyras, D., Barroso, L., Howarth, P., Wilkins, T., Rood, J.I. et al. (2002) Environmental response and autoregulation of Clostridium difficile TxeR, a sigma factor for toxin gene expression. *J Bacteriol* **184**: 5971-5978.

Margot, P., Wahlen, M., Gholamhoseinian, A., Piggot, P., and Karamata, D. (1998) The lytE gene of Bacillus subtilis 168 encodes a cell wall hydrolase. *J Bacteriol* **180**: 749-752.

Milohanic, E., Jonquieres, R., Cossart, P., Berche, P., and Gaillard, J.L. (2001) The autolysin Ami contributes to the adhesion of Listeria monocytogenes to eukaryotic cells via its cell wall anchor. *Mol Microbiol* **39**: 1212-1224.

Ohnishi, R., Ishikawa, S., and Sekiguchi, J. (1999) Peptidoglycan hydrolase LytF plays a role in cell separation with CwlF during vegetative growth of Bacillus subtilis. *J Bacteriol* **181**: 3178-3184.

Olling, A., Seehase, S., Minton, N.P., Tatge, H., Schroter, S., Kohlscheen, S. et al. (2012) Release of TcdA and TcdB from Clostridium difficile cdi 630 is not affected by functional inactivation of the tcdE gene. *Microb Pathog* **52**: 92-100.

Peng, Z., Wang, S., Gide, M., Zhu, D., Lamabadu Warnakulasuriya Patabendige, H.M., Li, C. et al. (2018) A Novel Bacteriophage Lysin-Human Defensin Fusion Protein Is Effective in Treatment of Clostridioides difficile Infection in Mice. *Front Microbiol* **9**: 3234.

Perez, J., Springthorpe, V.S., and Sattar, S.A. (2011) Clospore: a liquid medium for producing high titers of semi-purified spores of Clostridium difficile. *J AOAC Int* **94**: 618-626.

Pilgrim, S., Kolb-Maurer, A., Gentschev, I., Goebel, W., and Kuhn, M. (2003) Deletion of the gene encoding p60 in Listeria monocytogenes leads to abnormal cell division and loss of actin-based motility. *Infect Immun* **71**: 3473-3484.

Popoff, M.R., and Bouvet, P. (2009) Clostridial toxins. *Future Microbiol* **4**: 1021-1064.

Popowska, M., and Markiewicz, Z. (2004) Murein-hydrolyzing activity of flagellin FlaA of Listeria monocytogenes. *Pol J Microbiol* **53**: 237-241.

Sebaihia, M., Wren, B.W., Mullany, P., Fairweather, N.F., Minton, N., Stabler, R. et al. (2006) The multidrug-resistant human pathogen Clostridium difficile has a highly mobile, mosaic genome. *Nat Genet* **38**: 779-786.

Sun, X., Wang, H., Zhang, Y., Chen, K., Davis, B., and Feng, H. (2011) Mouse relapse model of Clostridium difficile infection. *Infect Immun* **79**: 2856-2864.

Tasteyre, A., Barc, M.C., Collignon, A., Boureau, H., and Karjalainen, T. (2001) Role of FliC and FliD flagellar proteins of Clostridium difficile in adherence and gut colonization. *Infect Immun* **69**: 7937-7940.

Thwaites, J.J., and Mendelson, N.H. (1991) Mechanical behaviour of bacterial cell walls. *Adv Microb Physiol* **32**: 173-222.

Tuomanen, E., and Schwartz, J. (1987) Penicillin-binding protein 7 and its relationship to lysis of nongrowing Escherichia coli. *J Bacteriol* **169**: 4912-4915.

Vermassen, A., Talon, R., Andant, C., Provot, C., Desvaux, M., and Leroy, S. (2019) Cell-Wall Hydrolases as Antimicrobials against Staphylococcus Species: Focus on Sle1. *Microorganisms* **7**.

Vollmer, W., Joris, B., Charlier, P., and Foster, S. (2008) Bacterial peptidoglycan (murein) hydrolases. *FEMS Microbiol Rev* **32**: 259-286.

743 Voth, D.E., and Ballard, J.D. (2005) Clostridium difficile toxins: mechanism of action and role
744 in disease. *Clin Microbiol Rev* **18**: 247-263.
745 Wang, L., and Lin, M. (2008) A novel cell wall-anchored peptidoglycan hydrolase (autolysin),
746 IspC, essential for Listeria monocytogenes virulence: genetic and proteomic analysis.
747 *Microbiology* **154**: 1900-1913.
748 Wuenscher, M.D., Kohler, S., Bubert, A., Gerike, U., and Goebel, W. (1993) The iap gene of
749 Listeria monocytogenes is essential for cell viability, and its gene product, p60, has bacteriolytic
750 activity. *J Bacteriol* **175**: 3491-3501.
751 Wydau-Dematteis, S., El Meouche, I., Courtin, P., Hamiot, A., Lai-Kuen, R., Saubamea, B. et al.
752 (2018) Cwp19 Is a Novel Lytic Transglycosylase Involved in Stationary-Phase Autolysis
753 Resulting in Toxin Release in Clostridium difficile. *mBio* **9**.
754 Xu, Q., Chiu, H.J., Farr, C.L., Jaroszewski, L., Knuth, M.W., Miller, M.D. et al. (2014)
755 Structures of a bifunctional cell wall hydrolase CwlT containing a novel bacterial lysozyme and
756 an NlpC/P60 DL-endopeptidase. *J Mol Biol* **426**: 169-184.
757 Xu, Q., Mengin-Lecreulx, D., Liu, X.W., Patin, D., Farr, C.L., Grant, J.C. et al. (2015) Insights
758 into Substrate Specificity of NlpC/P60 Cell Wall Hydrolases Containing Bacterial SH3 Domains.
759 *mBio* **6**: e02327-02314.
760 Yamaguchi, H., Furuhata, K., Fukushima, T., Yamamoto, H., and Sekiguchi, J. (2004)
761 Characterization of a new Bacillus subtilis peptidoglycan hydrolase gene, yvcE (named cwlO),
762 and the enzymatic properties of its encoded protein. *J Biosci Bioeng* **98**: 174-181.
763 Zhu, D., Sorg, J.A., and Sun, X. (2018) Clostridioides difficile Biology: Sporulation,
764 Germination, and Corresponding Therapies for C. difficile Infection. *Front Cell Infect Microbiol*
765 **8**: 29.
766 Zhu, D., Bullock, J., He, Y., and Sun, X. (2019) Cwp22, a novel peptidoglycan cross-linking
767 enzyme, plays pleiotropic roles in Clostridioides difficile. *Environ Microbiol* **21**: 3076-3090.

768

769

770

771

772

773

774

775

776

777

778

Figure legends

Fig. 1. Construction of 0971 gene deletion mutant and analysis of growth profile and 0971 gene transcription.

A. Schematic representation of Cwl0971 structure. Cwl0971 contains a 27 amino acid signal peptide, and two main domains that are N-terminal 3 repeat bacterial SH3_3 domain (YgiM superfamily) and C-terminal NLPC/P60 catalytic domain.

B. Schematic representation of 0971 gene deletion and amplification in R20291. 1-F/R and 2-F/R were used as gene deletion verification primers; Primer 3-F/R were used for the full 0971 gene amplification.

C. Verification of 0971 deletion in R20291. M: 1 kb DNA ladder; 1: R20291 genome PCR test with primer 1-F/R; 2: R20291Δ0971 genome PCR test with primer 1-F/R; 3: R20291 genome PCR test with primer 2-F/R; 4: R20291Δ0971 genome PCR test with primer 2-F/R.

D. Analysis of growth profile.

E. Expression of 0971 gene during R20291 growth. Experiments were independently repeated thrice. Bars stand for mean ± SEM (*P < 0.05). One-way ANOVA was used for statistical significance.

Fig. 2. Effect of Cwl0971 defect on cell autolysis.

A. Triton X-100 autolysis assay.

B. LDH cytotoxicity assay.

C. Percent of dead cells.

D. Detection of cell viability. *C. difficile* cells were co-dyed with CFDA (green) / PI (red) and monitored by a fluorescent microscope at 40 × magnification. Experiments were independently repeated thrice. Bars stand for mean ± SEM (*P < 0.05, **P < 0.01). One-way ANOVA was used for statistical significance.

Fig. 3. Detection of Cwl0971 hydrolase activity with zymogram assay.

A. Zymogram assay. Purified Cwl0971 was used to detect hydrolase activity for the *B. subtilis* cell wall. Lane 1 was blank control. Quantity of Cwl0971 loaded in lane 1 was two folds of lane 2. Lysis was visualized as translucent zones appearing in the gel.

B. Western blotting. Zymogram was run in parallel with Western blot detection gels to confirm the proteins migrated at the correct size.

Fig. 4. Effect of Cwl0971 defect on toxin expression.

A. *tcdA* expression on transcription level.

B. *tcdB* expression on transcription level.

C. TcdA concentration in *C. difficile* supernatants.

D. TcdB concentration in *C. difficile* supernatants. Experiments were independently repeated thrice. Bars stand for mean ± SEM (*P < 0.05). One-way ANOVA was used for statistical significance.

Fig. 5. Effect of Cwl0971 defect on *C. difficile* physiology.

A. Sporulation assay. *C. difficile* strains were cultured in Clospore media for 120 h. Then, the cultures were 10-fold diluted and plated on BHIS plates with 0.1% TA to detect sporulation ratio.

B. Germination assay. The purified spores were diluted to OD_{600} of 1.0 in the germination buffer to detect the germination ratio. The boiled spores which were heated at 100 □ for 20 min were used as a negative control (without TA) for germination analysis.

C. Spores resistance to heat. 1×10^6 spores were used to detect spore resistance at 65 □ for 4 h.

D. Biofilm formation assay. Biofilm formation of *C. difficile* strains was detected at 24 and 48 h, respectively.

E. Motility assay. 0.3% agar BHIS plates were used for swarming assay (cultured for 24 h) and 0.175% agar BHIS plates were used for swimming assay (cultured for 12 h).

F. Adhesion assay. The adhesion ability of *C. difficile* vegetative cells was determined on HCT-8 cells. Experiments were independently repeated thrice. Bars stand for mean ± SEM (*P < 0.05, **P < 0.01, ***P < 0.001, ****P < 0.0001). One-way ANOVA was used for statistical significance.

Fig. 6. Evaluation of Cwl0971 defect on *C. difficile* virulence in mice.

A. Mean relative weight changes.

B. Survival curve.

C. Diarrhea percentages.

D. *C. difficile* in feces.

E. TcdA titer of fecal sample.

F. TcdB titer of fecal sample. Bars stand for mean ± SEM (*P < 0.05, **P < 0.01, ***P < 0.001). Student's unpaired *t*-test was used for statistical significance. Animal survivals were analyzed by Kaplan-Meier survival analysis with a log-rank test of significance.

Table 1. Bacteria and plasmids utilized in this study.

Strains or plasmids	Genotype or phenotype	Reference
Strains		
E. coli DH5α	Cloning host	NEB
E. coli HB101/pRK24	Conjugation donor	Lab stock
E. coli BL21(DE3)	Expression host	NEB
BL21/pET28a-0971	BL21(DE3) containing pET28a-0971	This work
C. difficile R20291	Clinical isolate; ribotype 027	Lab stock
R20291Δ0971	R20291 deleted 0971 gene	This work
R20291-pMTL84153	R20291 containing blank plasmid pMTL84153	This work
R20291Δ0971-pMTL84153	R20291ΔW containing blank plasmid pMTL84153	This work
R20291Δ0971-C	R20291ΔW complemented with pMTL84153-0971	This work
Plasmids		
pDL1	AsCpfI based gene deletion plasmid	This work
pUC57-PsRNA	sRNA promoter template	This work
pDL1-0971	0971 gene deletion plasmid	This work
pMTL84153	Complementation plasmid	This work
pMTL84153-0971	pMTL84153 containing 0971 gene	This work

pET28a	Expression plasmid	NEB
pET28a-0971	0971 expression plasmid in *E. coli* BL21(DE3)	This work

Supplement files

Fig. S1. *C. difficile* swimming and swarming on BHIS plates.

A. Swarming analysis at 24 h with 0.3% agar BHIS plate. 1: R20291; 2: R20291Δ0971; 3: R20291Δ0971-C.

B. Swimming analysis at 12 h with 0.175% agar BHIS plate. 1: R20291; 2: R20291Δ0971; 3: R20291Δ0971-C.

C. Swarming analysis at 24 h with 0.3% agar BHIS-Tm plate. 1: R20291-PMTL84153; 2: R20291Δ0971-pMTL84153; 3: R20291Δ0971-C.

D. Swimming analysis at 12 h with 0.175% agar BHIS-Tm plate. 1: R20291-PMTL84153; 2: R20291Δ0971-pMTL84153; 3: R20291Δ0971-C.

878

879

880

881

882

883

884

885

886

887

888 **Table S1. Primers utilized in this study.**

Primer	Sequence (5' to 3')
gRNA-F	AAAGTTAAAAGAAGAAAATAGAAATATAATCTTTAATTTGAAAAGATTTA
gRNA-R	AAGTGGTTCATCTGAAGGTACATATCTACAAGAGTAGAAATTA ATGGT
Up-F	ATATGTACCTTCAGATGAACCACTTTAATTTCTACTCTTGTAGATGAGGTAAAGCGTAA GGAAGCAG
Up-R	TGCTACCTTATCACAATCAGAA
Down-F	AAGTTCTGATTGTGATAAGGTAGCAAAAACCATCTAGCGAAGAATCA
Down-R	CATGCTGATCTAGATTTCTCCATAG CCTGGTGCATAATTCCCCATA
1-F	TACAAGGGAAAAACTGTAG
1-R	TTAATAGAGTATGTAAAGAATGTG
2-F	TGGAGAGTGATTTCAAAATGAAG
2-R	TTAAATCCTCTGTATATCGTTTT
3-F	ATGACCATGATTACGAATTCGAGCTGTGATAGTAGTGAAGAAAGCT
3-R	CGCGTGACGTCGACTCTAGAGGATCCTAAACAAATCTTCTTGCACCA
4-F	GTTTAACTTTAAGAAGGAGATATACATGCACCATCACCATCACCACCTTGAAAAGGGA ACAGTAACA
4-R	CAGTGGTGGTGGTGGTGGTGCTCGA CTAAACAAATCTTCTTGCACC
Q-0971-F	AATGGAGTTACTGGATGG

Q-0971-R	AGCAGATGTTACCTTACC
Q-*tcdA*-F	GCGGAAATGGTAGAAATG
Q-*tcdA*-R	ATCAGGTGCTATCAATACTT
Q-*tcdB*-F	GTATTACCTAATGCTCCAA
Q-*tcdB*-R	CACCTTCATAGTTATCTCTT
16s-F	CCGTAGTAAGCTCTTGAA
16s-R	TGGTGTTCCTCCTAATATC

889

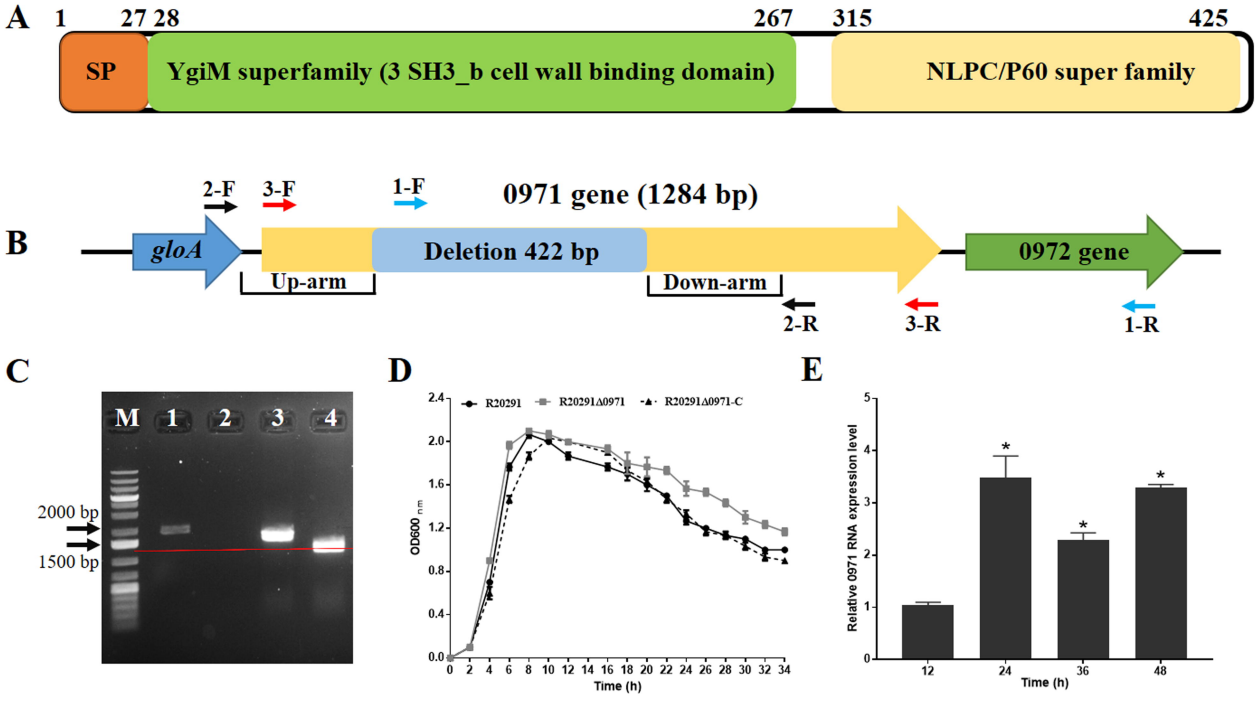
Cwl0971 protein (427 aa)
A
1
27 28
267
315
425
SP
YgiM superfamily (3 SH3_b cell wall binding domain)
NLPC/P60 super family
B
2-F
3-F
1-F
0971 gene (1284 bp)
gloA
Deletion 422 bp
0972 gene
Up-arm
Down-arm
2-R
3-R
1-R
C
M
1
2
3
4
2000 bp
1500 bp
D
R20291
R20291Δ0971
R20291Δ0971-C
OD600 nm
Time (h)
E
Relative 0971 RNA expression level
Time (h)

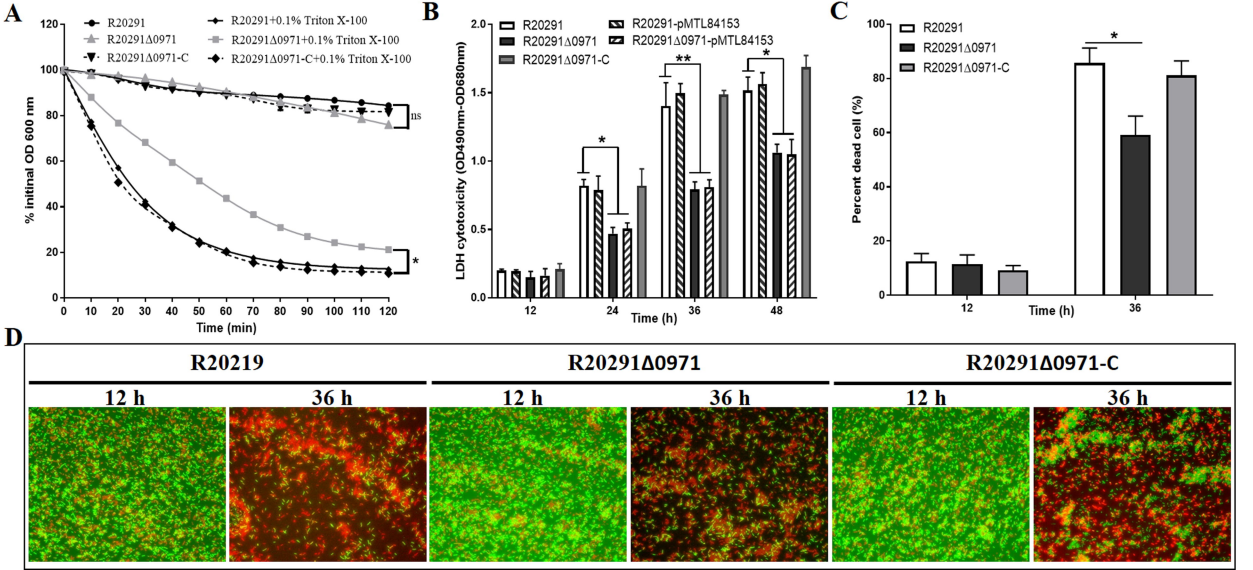
A
R20291
R20291Δ0971
R20291Δ0971-C
R20291+0.1% Triton X-100
R20291Δ0971+0.1% Triton X-100
R20291Δ0971-C+0.1% Triton X-100
% Initinal OD 600 nm
Time (min)
ns
*
B
R20291
R20291Δ0971
R20291Δ0971-C
R20291-pMTL84153
R20291Δ0971-pMTL84153
LDH cytotoxicity (OD490nm-OD680nm)
Time (h)
*
**
*
C
R20291
R20291Δ0971
R20291Δ0971-C
Percent dead cell (%)
Time (h)
*
D
R20219
R20291Δ0971
R20291Δ0971-C
12 h
36 h
12 h
36 h
12 h
36 h

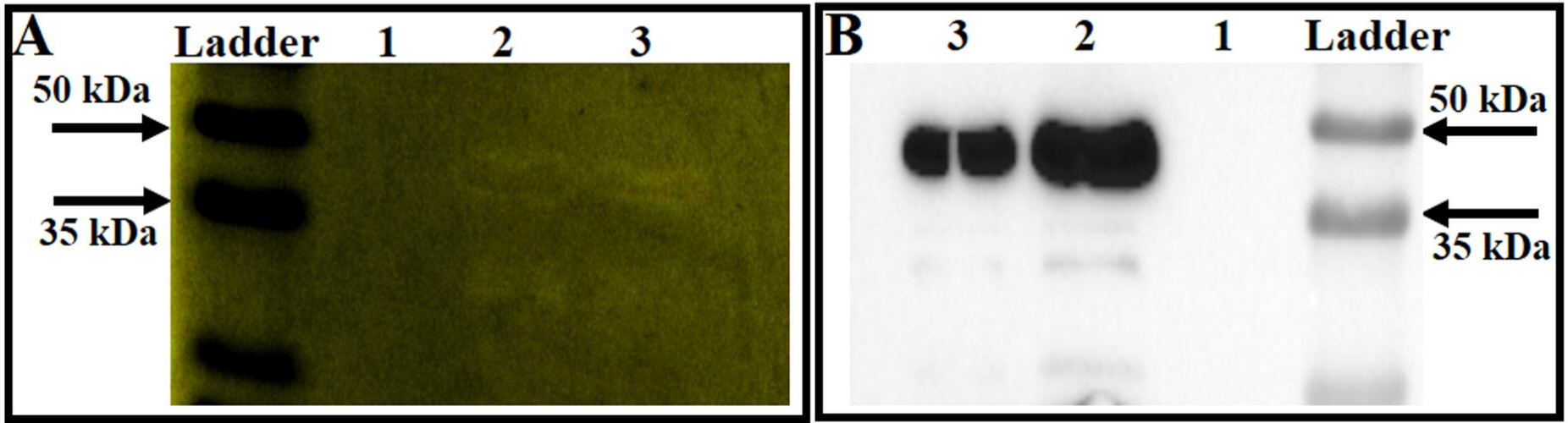
A
Ladder
1
2
3
50 kDa
35 kDa
B
3
2
1
Ladder
50 kDa
35 kDa

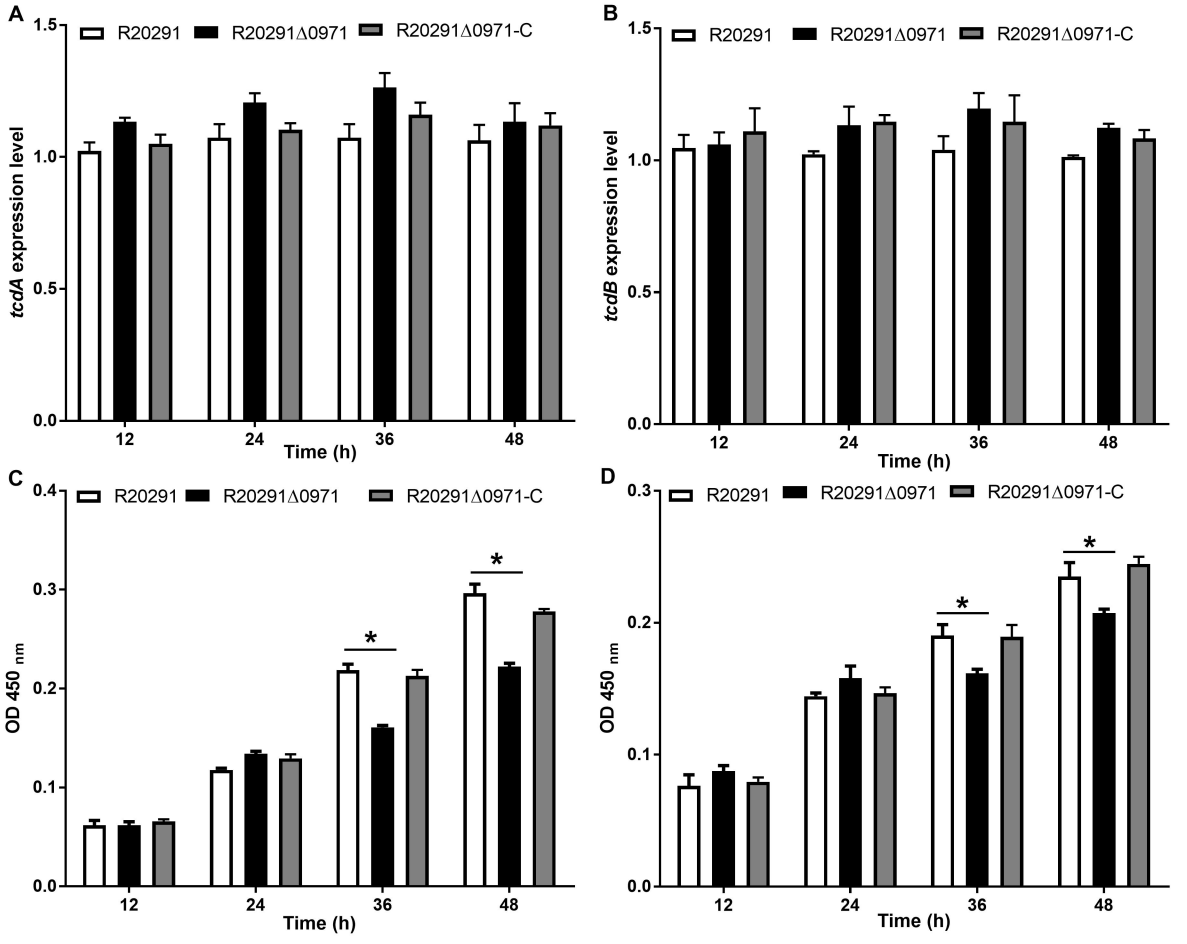
A
R20291
R20291Δ0971
R20291Δ0971-C
tcdA expression level
1.5
1.0
0.5
0.0
12
24
36
48
Time (h)
B
R20291
R20291Δ0971
R20291Δ0971-C
tcdB expression level
1.5
1.0
0.5
0.0
12
24
36
48
Time (h)
C
R20291
R20291Δ0971
R20291Δ0971-C
OD 450 nm
0.4
0.3
0.2
0.1
0.0
*
*
12
24
36
48
Time (h)
D
R20291
R20291Δ0971
R20291Δ0971-C
OD 450 nm
0.3
0.2
0.1
0.0
*
*
12
24
36
48
Time (h)

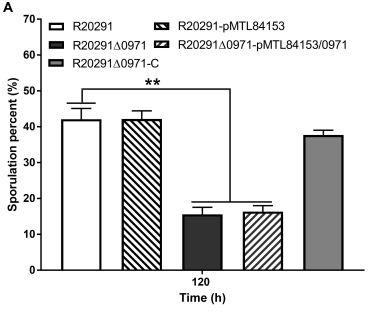
A
R20291
R20291-pMTL84153
R20291Δ0971
R20291Δ0971-pMTL84153/0971
R20291Δ0971-C
Sporulation percent (%)
**
120
Time (h)

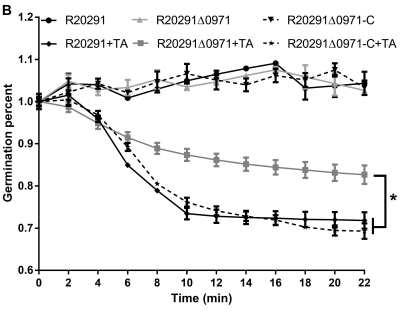
B
R20291
R20291Δ0971
R20291Δ0971-C
R20291+TA
R20291Δ0971+TA
R20291Δ0971-C+TA
Germination percent
Time (min)
*

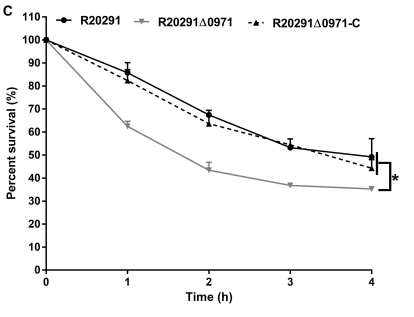
C
R20291
R20291Δ0971
R20291Δ0971-C
Percent survival (%)
Time (h)
*

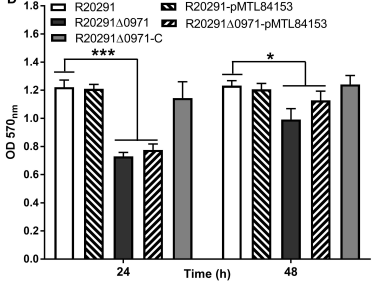
D
R20291
R20291-pMTL84153
R20291Δ0971
R20291Δ0971-pMTL84153
R20291Δ0971-C
OD 570nm
***
*
24
Time (h)
48

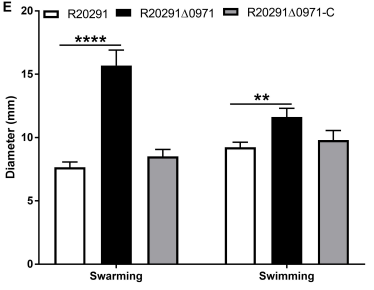
E
R20291
R20291Δ0971
R20291Δ0971-C
Diameter (mm)
****
**
Swarming
Swimming

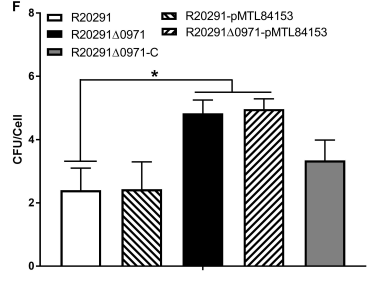
F
R20291
R20291-pMTL84153
R20291Δ0971
R20291Δ0971-pMTL84153
R20291Δ0971-C
CFU/Cell
*

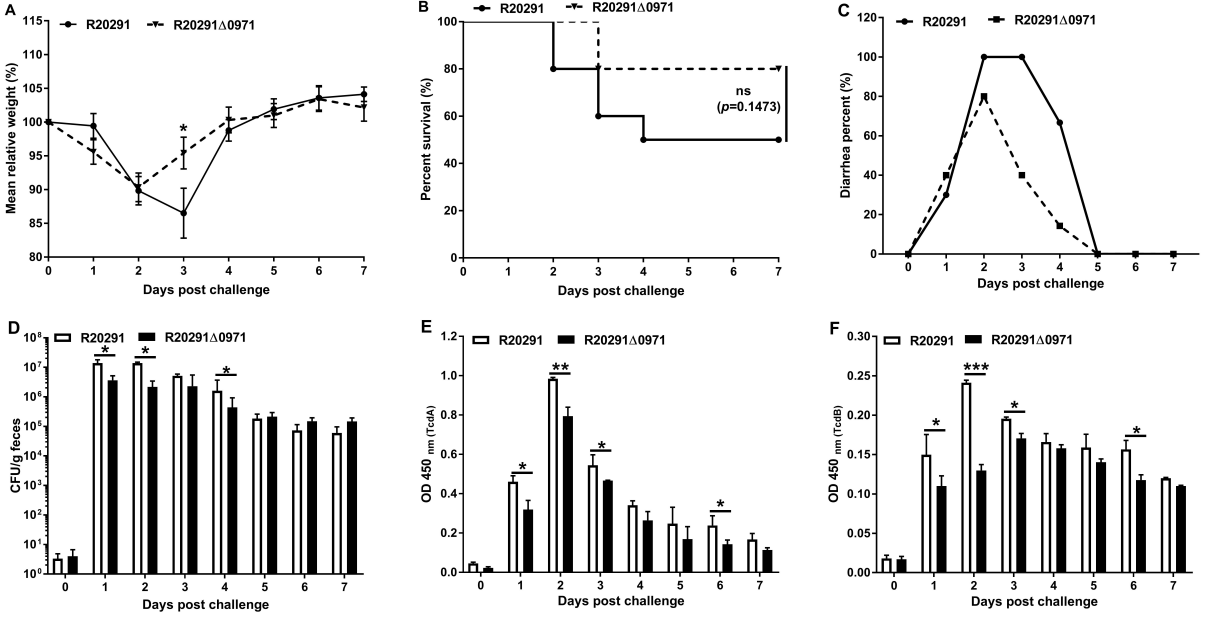
A
R20291
R20291Δ0971
Mean relative weight (%)
Days post challenge
B
R20291
R20291Δ0971
Percent survival (%)
ns
(p=0.1473)
Days post challenge
C
R20291
R20291Δ0971
Diarrhea percent (%)
Days post challenge
D
R20291
R20291Δ0971
CFU/g feces
Days post challenge
E
R20291
R20291Δ0971
OD 450 nm (TcdA)
Days post challenge
F
R20291
R20291Δ0971
OD 450 nm (TcdB)
Days post challenge